Original Article

Mixotrophy in the bloom-forming genus *Phaeocystis* and other haptophytes

Sebastiaan Koppelle [a,*], David López-Escardó [b], Corina P.D. Brussaard [a,c], Jef Huisman [a], Catharina J.M. Philippart [d,e], Ramon Massana [b], Susanne Wilken [a,*]

[a] *Department of Freshwater and Marine Ecology (FAME), Institute for Biodiversity and Ecosystem Dynamics (IBED), University of Amsterdam, P.O. Box 94920, 1090 XH, Amsterdam, The Netherlands*
[b] *Ecology of Marine Microbes, Institut de Ciènces del Mar (ICM-CSIC), Passeig Marítim de la Barceloneta 37-49, 08003 Barcelona, Catalonia, Spain*
[c] *Department of Marine Microbiology and Biogeochemistry, NIOZ Royal Netherlands Institute for Sea Research, P.O. Box 59, 1790 AB, Den Burg, Texel, The Netherlands*
[d] *Department of Coastal Systems, NIOZ Royal Netherlands Institute for Sea Research, P.O. Box 59, 1790 AB, Den Burg, Texel, The Netherlands*
[e] *Department of Physical Geography, Utrecht University, P.O. Box 80115, 3508 TC, Utrecht, The Netherlands*

ARTICLE INFO

ABSTRACT

Phaeocystis is a globally widespread marine phytoplankton genus, best known for its colony-forming species that can form large blooms and odorous foam during bloom decline. In the North Sea, *Phaeocystis globosa* typically becomes abundant towards the end of the spring bloom, when nutrients are depleted and the share of mixotrophic protists increases. Although mixotrophy is widespread across the eukaryotic tree of life and is also found amongst haptophytes, a mixotrophic nutrition has not yet been demonstrated in *Phaeocystis*. Here, we sampled two consecutive *Phaeocystis globosa* spring blooms in the coastal North Sea. In both years, bacterial cells were observed inside 0.6 – 2% of *P. globosa* cells using double CARD-FISH hybridizations in combination with laser scanning confocal microscopy. Incubation experiments manipulating light and nutrient availability showed a trend towards higher occurrence of intracellular bacteria under P-deplete conditions. Based on counts of bacteria inside *P. globosa* cells in combination with theoretical values of prey digestion times, maximum ingestion rates of up to 0.08 bacteria cell^{-1} h^{-1} were estimated. In addition, a gene-based predictive model was applied to the transcriptome assemblies of seven *Phaeocystis* strains and 24 other haptophytes to assess their trophic mode. This model predicted a phago-mixotrophic feeding strategy in several (but not all) strains of *P. globosa, P. antarctica* and other haptophytes that were previously assumed to be autotrophic. The observation of bacterial cells inside *P. globosa* and the gene-based model predictions strongly suggest that the phago-mixotrophic feeding strategy is widespread among members of the *Phaeocystis* genus and other haptophytes, and might contribute to their remarkable success to form nuisance blooms under nutrient-limiting conditions.

1. Introduction

Oxygenic photosynthesis performed by phytoplankton represents roughly 50% of the global primary production (Field et al., 1998). Moreover, phytoplankton represent an important food source for zooplankton, which are in turn consumed by higher trophic levels. However, several factors can complicate this traditional view of photosynthetic phytoplankton as the basis of the food web. Non-edible harmful algal species, viral lysis as significant loss factor, and mixotrophic protists that combine photosynthetic carbon fixation (photo-autotrophy) with a heterotrophic nutrition all redirect the flow of energy and matter (Weisse et al., 1994; Schoemann et al., 2005; Brussaard et al., 2005a; Mitra et al., 2014).

Mixotrophy has been known for almost a century (Pascher, 1917; Hofeneder, 1930), but its wider ecological relevance in aquatic ecosystems has only been recognized during the last decades (Bird and Kalff, 1986; Zubkov and Tarran, 2008; Flynn et al., 2013). The ability to ingest prey via phagocytosis is an ancient eukaryotic trait that was involved in the evolutionary acquisition of photosynthetic endosymbionts. The earliest photosynthetic eukaryotes have thus combined photosynthesis with phagocytosis of microbial prey and such a phago-mixotrophic strategy is still widespread among protists across the eukaryotic tree of life (Stoecker et al., 2017; Worden et al., 2015). Many species traditionally considered obligate photoautotrophs continue to be identified as mixotrophs, including recent examples from diverse eukaryotic supergroups (Avrahami and Frada, 2020; Bock et al., 2021; Gerea et al.,

* Corresponding authors.
  E-mail addresses: s.koppelle@uva.nl (S. Koppelle), s.wilken@uva.nl (S. Wilken).

2013). Although maintaining both the photosynthetic and phagocytic machinery is assumed to be energetically costly (Raven, 1997), mixotrophy can be of considerable advantage in comparison to purely photoautotrophic growth, because it provides access to particulate nutrients bound in bacteria or algal prey in situations where dissolved inorganic nutrients or light are limiting (Flynn et al., 2019 and references therein).

Mixotrophs are commonly encountered in oligotrophic systems (Jones, 2000), but also dense harmful algal blooms (HABs) in eutrophic coastal waters can be dominated by mixotrophic protists (Burkholder et al., 2008 and references herein). For example, mixotrophy has been found among a variety of HAB-forming dinoflagellates (e.g., Stoecker, 1999; Burkholder et al., 2008), the raphidophyte genera *Chatonella* and *Heterosigma* (Nygaard and Tobiesen, 1993; Seong et al., 2006) and the haptophytes *Prymnesium parvum* and *Chrysochromulina* spp. (Legrand et al., 2001; Nygaard and Tobiesen, 1993). These mixotroph-dominated HABs are thought to be the result of the transition from a nutrient replete and autotroph dominated system during spring, towards a summer situation characterized by depleted nutrient conditions and enhanced availability of dissolved and particulate organic matter (Mitra et al., 2014). Feeding on prey could lift potential nutrient limitation or stoichiometric imbalances, thereby stimulating and sustaining the growth of mixotrophic HABs (Burkholder et al., 2008; Flynn et al., 2018).

The globally widespread genus *Phaeocystis* represents a group of ecologically important haptophytes for which the possibility of mixotrophy has occasionally been suggested (e.g., Gast et al., 2018; Rizkallah et al., 2020), but not yet demonstrated. Species within this genus are typically able to form (large) colonial blooms in coastal waters from the poles to the tropics, which upon decay can support high bacterial production (Brussaard et al., 2005b; Schoemann et al., 2005). The colony forming species *P. globosa* is considered a HAB-forming species (Veldhuis and Wassmann, 2005), because its colonial stage can cause clogging of fishing nets (Savage, 1930), its production of toxic metabolites has been linked to mass mortality of cultured fish (Huang et al., 1999), and the demise of *P. globosa* blooms results in large amounts of odorous foam washing ashore (Lancelot, 1995; Blauw et al., 2010). In the southern North Sea yearly recurring blooms of *P. globosa* typically occur between late March and June, right after the diatom spring bloom (Cadée and Hegeman, 2002; Schoemann et al., 2005). Although nutrients often become depleted during this period (Burson et al., 2016), *P. globosa* is still able to form high density blooms. Under such conditions, mixotrophy may provide an alternative route of nutrient acquisition from prey, and thereby contribute to *Phaeocystis'* success as a HAB forming species.

Here, we examine the potential occurrence of mixotrophy in a natural bloom of *P. globosa* in the southern coastal North Sea. Double CARD-FISH assays in combination with laser-scanning confocal microscopy were performed to detect bacteria-containing vacuoles inside *P. globosa* cells. Subsequently, an incubation experiment was performed to test the impact of light and nutrient manipulation on the potential grazing by *Phaeocystis* during a bloom period. Finally, to extend the field observations to a wider diversity of haptophytes, a gene-based model (Burns et al., 2018) was applied to the transcriptome assemblies of seven *Phaeocystis* strains and 24 other haptophytes to assess their phototrophic and phagotrophic capabilities and, hence, to predict their trophic mode.

2. Materials and methods

To gain insight into the *Phaeocystis* bloom development and its dynamics in the North Sea, we made use of the long-term time series program of the Royal Netherlands Institute for Sea Research (NIOZ) (Philippart et al., 2000; Jacobs et al., 2020) for both the 2019 and 2020 spring bloom periods (January – July). This provided weekly to biweekly samples for nutrient and chlorophyll *a* concentrations, as well as *P. globosa* abundances (section 2.1). Additionally, phytoplankton community composition was characterized for the smaller size fraction

(< 70 μm) expected to include bacterivorous protists (section 2.2), and *P. globosa* was assessed for potential bacterivory using CARD-FISH (section 2.3) once in May 2019 and over a three-month period (April to early July) in 2020. Furthermore, *P. globosa* was sampled for an incubation experiment performed in May 2019 to investigate environmental drivers influencing bacterivory in *P. globosa* (section 2.6).

2.1. Monitoring of Phaeocystis dynamics

To obtain information on *P. globosa* bloom dynamics during two consecutive spring blooms in 2019 and 2020 (January – July), surface water was collected from the monitoring platform of the NIOZ located at the Marsdiep tidal inlet at the island of Texel, the Netherlands (53°00′06.5″N, 4°47′20.6″E). Water samples were collected using bucket tows during high tide and analyzed for dissolved inorganic nutrient and chlorophyll *a* concentrations as described by Jacobs et al. (2020). Water samples were gently filtered over a 0.22 μm polyethersulfone filter (PES, VWR®, Radnor, PA, US). Filtered samples were stored at -20 °C for dissolved inorganic nitrogen (DIN, i.e. $NO_x + NH_4^+$) and dissolved inorganic phosphorus (DIP), and at 4 °C for silicate (Si), until analysis on a SEAL TrAAcs800 autoanalyzer at the NIOZ (SEAL Analytical Netherlands, the Netherlands; mean detection limits: DIP = 0.007 μmol L^{-1}, NO_x = 0.022 μmol L^{-1}, NH_4^+ = 0.010 μmol L^{-1}, Si = 0.024 μmol L^{-1}; Murphy and Riley, 1962, Helder and de Vries, 1979; Grasshoff et al., 1983, Strickland and Parsons, 1968). For chlorophyll *a*, 250–500 mL water samples were filtered onto GF/F filters (Whatman®, 47 mm diameter), shock-frozen (in liquid nitrogen) and stored at −80 °C until extraction and processing using high performance liquid chromatography (HPLC) as described by Evans et al. (1975). Water samples (100 ml) for *Phaeocystis* abundance were fixed with 300 μl of alkaline Lugol's solution, and stored in the dark at 4 °C until further analysis. Cells were counted within viewing fields after sedimentation in 3.25-mL counting chambers at different levels of magnification (58 fields at 10 × 100, 70 fields at 10 × 40, 29 fields at 10 × 10, and a complete count of the chamber at 10 × 10 magnification) using an Olympus (MT2) inverted microscope. For the haptophyte *Phaeocystis* spp., which mainly consisted of *P. globosa*, the two life forms (colony and flagellate cells, recognizable by their morphology and the respective absence and presence of flagella) were counted separately but their cell numbers were summed for this study.

2.2. Phytoplankton community composition

Phytoplankton community composition samples were collected in a similar manner as described in 2.1 with the exception that collected water was first filtered over a 70 μm mesh to remove large *Phaeocystis* colonies and zooplankton grazers. Samples (45 mL) were preserved with acidic Lugol's (1% v/v final concentration) and stored at 4 °C in the dark until analysis using an inverted light microscope (Zeiss IM35, Utermöhl method). Briefly, samples were checked for cell density and concentrated via sedimentation if needed to achieve high enough density for counting. Samples were then transferred to a counting chamber (1 mL), allowed to settle, and 200–300 cells were identified to the highest phylogenetic resolution possible and counted per sample. Cellular biovolumes were estimated from measurements of cellular dimensions at 250 and 600x magnification according to "Zellformen - Phytoplankton: Externe Qualitätssicherung bei EQAT Phytoplankton" (www.planktonforum.eu). For each taxon, as many cells were measured as needed until the standard error of the mean measured biovolume was less than 10%. Cells were grouped by class and *P. globosa* was counted as a separate group.

2.3. Catalyzed reporter deposition fluorescence in situ hybridization (CARD-FISH)

To detect potential bacteria-containing vacuoles inside *P. globosa*

cells, CARD-FISH samples from the incubation experiment in 2019 (see below, section 2.6) and ten time points between April and July in 2020 were collected, fixed with 0.2 μm filtered 37% formaldehyde (3.7% final concentration) and incubated overnight in the dark at 4 °C. Following, 15 mL of sample was filtered over 3 μm pore-size polycarbonate filters (PC, 25 mm diameter, Whatman®, GE Healthcare, Life Science, US), air dried and kept frozen at -80 °C until further processing. To allow dual visualization of both *P. globosa* and bacteria, a double CARD-FISH assay was performed as described before (Pernthaler and Amann, 2004; Piwosz et al., 2021). For targeting *Phaeocystis*, the *Phaeocystis*-specific probe Phaeo02 was used at a final concentration of 5 ng μL^{-1} (Table 1, 18S rRNA targeted; Zingone et al., 1999). After hybridization, *P. globosa* signal was amplified with Alexa Fluor™ 555 labeled tyramide (Invitrogen™, Thermo Fisher Scientific, US) and 4-iodophenylboronic acid (IPBA, 20 mg mL^{-1}) was added to the labelled fluorophore solution to enhance the signal (Bobrow et al., 2002; Pernthaler and Amann, 2004). Before continuing with the additional CARD-FISH hybridization, peroxidases were inactivated by incubating the filter in 0.01 mol L^{-1} HCl for 10 min at room temperature.

To target the bacteria, a second CARD-FISH hybridization was performed using a mix of the probes CF319a (16S rRNA targeted, Manz et al., 1996), Gam42a and the competitor probe Bet42a (23S rRNA targeted, Manz et al., 1992) to target members of the *Cytophaga--Flavobacteria* and the *γ-Proteobacteria*, respectively (final concentration of 0.17 ng μL^{-1}; Table 1). Combining these two probes represented approximately 50% of the prokaryotic community in our sample based on relative read abundances obtained from 16S amplicon sequencing (data not shown, pers. comm. Dr. J. Engelmann, NIOZ). Alexa Fluor™ 488 labeled tyramide (Invitrogen™, Thermo Fisher Scientific, US) was used to amplify the bacterial signal. After the final washing steps, filters were air dried, mounted on microscope glass slides using an antifade mounting medium with DAPI (VECTASHIELD®, H-1200, Vector Laboratories, US) and stored at -20 °C until further analysis.

2.4. Probe specificity

To rule out any potential probe hybridization to non-target mitochondrial or plastidial rRNA of eukaryotic phytoplankton and more specifically *P. globosa*, the specificity of the probes was tested. First, the probes Gam42a/Bet42a and CF319a were tested for potential matches by running them against the Silva large subunit 132 (LSU, 23S) and small subunit 138 (SSU, 16S) databases (https://www.arb-silva.de/search/testprobe/, Quast et al., 2013). Subsequently, the CF319a probe sequence was used to BLAST against a plastidial 16S rRNA sequence database (PhytoREF, Decelle et al., 2015) with a 100% sequence similarity. No significant matches with either mitochondria or chloroplast related sequences were found.

The specificity of the Phaeo02 probe for targeting *Phaeocystis* was already shown by Zingone et al. (1999), and confirmed by a BLAST run of the probe sequence against the V4 18S rRNA sequences obtained from amplicon sequencing analysis of the experimental community collected in 2019 (raw sequencing data is available from the NCBI Sequence Read Archive (SRA) under accession PRJNA849788 (https://www.ncbi.nlm.

nih.gov/bioproject/849788), see also 'Texel_seqs.fasta' in the supplementary material). As a last check we used an axenic culture of *P. globosa* Pg-G (A) as a positive control for the *Phaeocystis* probe and a negative control for the prokaryotic probes (Gam42a/Bet42a, CF319a) performing separate single CARD-FISH hybridizations. Briefly, an exponential growing culture (L1 medium (Guillard and Hargraves, 1993) supplemented with 150 μmol L^{-1} NH$_4$Cl; 15 °C; 80 μmol photons $m^{-2} s^{-1}$; 16:8 h light:dark light cycle) was first checked for axenicity. For this, a subsample of the *P. globosa* culture was filtered onto 0.2 μm pore-size polycarbonate filters (PC, 25 mm diameter, Whatman®, GE Healthcare, Life Science, United States), counter-stained with a DAPI containing antifade mounting medium (VECTASHIELD®) and screened for the presence of bacterial cells at 1000x magnification on a Zeiss Axioskop 2 epifluorescence microscope. Subsequently, samples for CARD-FISH were obtained and processed as described in section 2.3. These tests confirmed the suitability of the *Phaeocystis* probe and the absence of any false positive signals from the prokaryotic probes within *P. globosa* cells.

2.5. Confocal microscopy

CARD-FISH samples were examined at 600x magnification using a laser scanning confocal microscope (Nikon A1r) with appropriate filter sets at the van Leeuwenhoek center for Advanced Microscopy (LCAM, http://www.lcam-fnwi.nl/lcam/, University of Amsterdam). Per sample ~300 *P. globosa* cells were counted adding up to a total of ~900 cells per treatment. To detect and confirm potential ingestion events, *P. globosa* cells with associated bacteria were selected and Z-stacks consisting of 15–21 images (~0.35 μm steps) were collected and used to generate final images and 3D animations. Further processing of images and movies was done in the Fiji package of ImageJ (Schindelin et al., 2012). The *Phaeocystis*-bacteria associations were then distinguished based on the location of the bacteria being (i) on the exterior of the *P. globosa* cell (not counted), (ii) being clearly inside the *P. globosa* cell (counted as confirmed intracellular bacteria), or (iii) appearing to be inside the *P. globosa* cell, but with the localization not being visible clearly enough to be confidently classified as intracellular (counted as likely intracellular bacteria; see Supplementary Figure S1 for examples).

2.6. Incubation experiment

An incubation experiment was performed to assess the impact of light and nutrient availability on potential bacterial prey ingestion by *P. globosa*. For this, surface water was collected during the early morning on the 2nd of May 2019, gently sieved over a 200 and 70 μm mesh to remove large colonies in which we did not expect to observe feeding, and transferred to 4 L polycarbonate incubation bottles (Nalgene™, Thermo Fisher Scientific, US). Light and nutrient conditions were manipulated in a full factorial design leading to four treatments, each performed in triplicate: Control (*in situ* nutrient availability and incubation in the light), +N + P (addition of 10 μmol L^{-1} K$_2$HPO$_4$ and 160 μmol L^{-1} NaNO$_3$ and incubation in the light), dark (*in situ* nutrient availability and incubation in darkness), and a combination of dark and +N + P. Bottles were incubated in a climate room at 12 °C and light

Table 1
Oligonucleotide probe sequences, specificity, target sites and formamide concentrations in the hybridization buffer (HB). All probes used were ligated to a horseradish peroxidase (HRP) molecule on their 5′ end (except for competitor probe Bet42a).

Probe	Specificity	Sequence	Target site rRNA positions	% Formamide in HB	Reference
Gam42a	*γ-Proteobacteria*	5′-GCCTTCCCACATCGTTT-3′	23S, 1027 – 1043[a]	55	Manz et al. (1992)
Bet42a	*β-Proteobacteria*	5′-GCCTTCCCACTTCGTTT-3′	23S, 1027 – 1043[a]	55	Manz et al. (1992)
CF319a	*Cytophaga-Flavobacteria (Bacteroidetes)*	5′-TGGTCCGTGTCTCAGTAC-3′	16S, 319 – 336[a]	55	Manz et al. (1996)
Phaeo02	*Phaeocystis*	5′-TCGGCAGACCGCTCGGCCCG-3′	18S, 647 – 666[b]	50	Lange et al. (1996) Zingone et al. (1999)

[a] Based on *E.coli* numbering as in Brosius et al. (1981).
[b] Based on positions as in Zingone et al. (1999).

treatments received ~64 μmol photons $m^{-2}\,s^{-1}$ with a 15:9 h light:dark cycle to simulate *in situ* light conditions. For dark incubations bottles were wrapped in light proof black bags (508 × 762 mm, #94915, Toolstation, Bridgwater, UK). All bottles were incubated for 24 h and manually mixed by careful rotation every 6 h. Samples for the dissolved inorganic nutrient concentrations and phytoplankton community composition (Lugol's preserved samples) were taken at the start of the experiment as described above. Samples for CARD-FISH were collected after 6 and 18 h of incubation (corresponding to noon and midnight) to determine potential ingestion of natural bacterial prey by *Phaeocystis* (see section 2.3).

2.7. Statistical analysis of incubation experiment

To analyze the effect of nutrient addition and dark incubation on the percentage of *Phaeocystis* cells containing bacteria, a two-way ANOVA was performed. To test for a potential relation between the diel cycle and prey inside *Phaeocystis*, percentages of *Phaeocystis* cells containing bacteria at noon were compared to those at midnight for the control treatment using a two-tailed Student's *t*-test. A significance level of $p = 0.05$ was used and data are presented as averages with 1 standard deviation. All analyses were performed in R Studio (version 1.4.1106) and SigmaPlot 14.

2.8. Predicting trophic modes: gene-based predictive model

The trophic strategy of a variety of haptophyte strains was predicted using the gene-based model developed by Burns et al. (2018). Briefly, this model is based on protein clusters derived from the eukaryotic genomes of 35 taxa and construction of hidden Markov models (HMMs) from those 14,095 protein clusters that contained proteins from at least three taxa. From this total set, 474 protein clusters were enriched in phagotrophs versus non-phagotrophs and 243 protein clusters were enriched in phototrophs versus non-phototrophs. These protein clusters were further categorized functionally based on their Gene Ontology (GO) biological processes. Organisms were scored on their completeness of these GO categories, and feature selection based on random forests retained only those GO categories predictive of the trophic strategy. Finally, these were used to train a probability neural network classifier to predict trophic modes. Many of the 474 protein clusters predictive of phagotrophy were absent in the phagotrophic parasites *Entamoeba histolytica* (367 protein clusters absent from generalist model) and *Rozella allomycis* (397 protein clusters absent from the generalist model), due to genome reduction in these parasitic species. Therefore, two additional predictive models were constructed based on a smaller set of protein clusters conserved in these parasites (111 and 84 proteins, respectively). Burns et al. (2018) validated their model using 112 genomes and transcriptomes from eukaryotes of known trophic strategy, and found that photosynthetic and phagotrophic capabilities were correctly predicted for all free-living eukaryotes in their study. Both the training and validation data set contained a diversity of eukaryotes including one and two haptophyte taxa, respectively. Here we first applied the full predictive model, and in cases where this did not predict phagotrophic capability, the *R. allomycis* model was used subsequently. All code was derived from Burns et al. (2018, https://github.com/burnsajohn/predictTrophicMode), where a more detailed description of the model can be found.

To predict the trophic strategy of 31 haptophyte strains we used predicted protein sequences from the two genomes of *Emiliania huxleyi* CCMP1516 (Read et al., 2013, https://genome.jgi.doe.gov/portal/Emihu1/Emihu1.download.html) and *Chrysochromulina tobin* CCMP 291 (Hovde et al., 2015, https://genome.jgi.doe.gov/portal/Chrsp_1/Chrsp_1.download.html), as well as 29 transcriptome assemblies. These transcriptomes included seven *Phaeocystis* and 22 other haptophyte strains, covering the major lineages within the haptophytes including the haptophytes from the training and validation set of Burns et al. (2018) (Supplementary Table S1). The majority of the transcriptomes were obtained from the Marine Microbial Eukaryote Transcriptome Sequencing project (MMETSP; Keeling et al., 2014; https://www.imicrobe.us/#/projects/104), with the exception of *P. globosa* CCMP1528 and *P. antarctica* Rizkallah, which were obtained elsewhere (Brisbin and Mitarai, 2019; Rizkallah et al., 2020). Transcriptome completeness was determined with BUSCO v3.0.2 (Waterhouse et al., 2018) using the eukaryotic database OrthoDB v9 (Zdobnov et al., 2017). Strains with less than 60% completeness were excluded from the analysis.

2.9. Phylogenetic analysis

A phylogenetic tree of the strains included in the gene-based predictive model was reconstructed based on 18S rRNA gene sequences. Sequences were obtained either from the MMETSP metadata files, or retrieved from transcriptome assemblies by BLAST (Altschul et al., 1990), using 18S rRNA gene sequences of the PR2 database (Guillou et al., 2013) as query. As an outgroup, 18S rRNA sequences of 5 katablepharid species (*Leucocryptos marina* clone 3902, *Hatena arenicola* HY-051, *Katablepharis japonica* AB231617, *K. remigera* AY919672, uncultured Katablepharid KF761288) were obtained from the PR2 database. Sequences were aligned in MEGA X (Kumar et al., 2018) using ClustalW and cut to a total length of 1370 bp. Comparison of the maximum likelihood fits of 24 different nucleotide substitution models using the Bayesian Information Criterion (BIC) showed that the Tamura-Nei (TN93) nucleotide substitution model with a discrete gamma distribution (G) and evolutionary invariable sites (I) provided the best description of the substitution patterns. Hence, this substitution model was used to compute a maximum likelihood phylogenetic tree in MEGA X (Kumar et al., 2018). Gaps were treated as complete deletion. The tree was based on 500 bootstrap replicates and rooted on the outgroup.

3. Results

3.1. Phaeocystis bloom development

For both 2019 and 2020, similar trends in chlorophyll *a* concentration, *Phaeocystis* bloom development, and dissolved inorganic nutrient concentrations were observed (Fig. 1). For both years chlorophyll *a* concentrations of ~2 μg L^{-1} were measured in January, followed by a gradual increase until the end of March after which chlorophyll *a* concentrations steeply increased to maximum values of ~23 μg L^{-1} in mid-April. This peak in chlorophyll *a* was followed by a peak in *Phaeocystis* abundance (Fig. 1A,D), with maximum *Phaeocystis* abundances towards the end of April. Although bloom dynamics were similar in both years, *Phaeocystis* displayed a higher peak abundance in 2020 (42.4 × 10^3 cells mL^{-1}) than in 2019 (27.7 × 10^3 cells mL^{-1}). After the peak, the *Phaeocystis* abundance decreased during May and was reduced to < 1% of its peak abundance by the end of that month.

In both years the phytoplankton spring bloom was accompanied by nutrient depletion (Fig. 1B,E). Briefly, the DIN concentration decreased from peak values of ~ 70 μmol L^{-1} at the end of March to < 3 μmol L^{-1} by the end of April. The DIP concentration remained relatively stable at 0.5–0.7 μmol L^{-1} until early March, and then decreased by an order of magnitude to 0.05–0.06 μmol L^{-1} in early April. The silicate concentration showed similar dynamics as DIP, with a strong drawdown from mid-March to early April, although silicate was depleted to a much lower concentration in April 2020 than in April 2019 (0.3 μmol L^{-1} versus 4 μmol L^{-1}).

3.2. Phytoplankton community composition

On the day of the incubation experiment (2nd of May 2019) *Phaeocystis* dominated the phytoplankton community in the <70 μm size fraction (80% based on biovolume), followed by Bacillariophyceae (7.0%) and Cryptophyceae (3.4%). The numerical abundance of
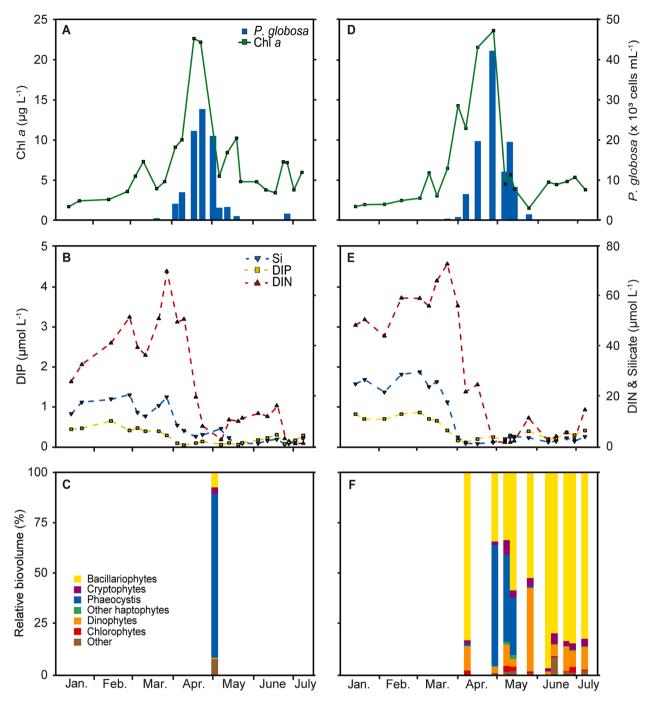
Fig. 1. *P. globosa* bloom dynamics during the time-series sampling in 2019 (A, B, C) and 2020 (D, E, F; January – July). (A, D) Chlorophyll *a* concentration and *P. globosa* abundance as measured at the NIOZ monitoring jetty during high tide. (B, E) Dissolved inorganic phosphorus (DIP), nitrogen (DIN), and silicate (Si) concentrations. (C, F) Phytoplankton community composition (based on relative biovolume) in the < 70 μm size fraction. Low abundant taxa (e.g. dictyochophytes, euglenophytes, chrysophytes and cyanobacteria) were grouped together in the 'other' category.

P. globosa in this small size fraction was $21.0 \pm 0.1 \times 10^3$ cells mL^{-1}, which comprised ~76% of the total *Phaeocystis* abundance in that sample (see Fig. 1A)

In 2020, phytoplankton biovolumes were assessed from the 7th of April onwards. In early April, *Phaeocystis* abundance was still relatively low (0.3×10^3 cells mL^{-1}) and contributed only 1% of the total phytoplankton biovolume in the < 70 μm size fraction, while diatoms dominated with 83% (Fig. 1F). By the end of April, the share of *Phaeocystis* had increased to 60% of the phytoplankton biovolume. Thereafter, the *Phaeocystis* contribution was >30% until the 11th of May with abundances between 1.5 and 6.1×10^3 cells mL^{-1}. In the second half of

May, *Phaeocystis* strongly declined (0.8% of biovolume on 25th of May), and diatoms became dominant with smaller contributions by dinoflagellates and cryptophytes during the subsequent summer months. While the *Phaeocystis* bloom progressed, an increasing part of the *Phaeocystis* was retrieved in the <70 μm size fraction (Table 2), suggesting that the population largely consisted of single cells and small colonies towards the end of the bloom.

3.3. Detection of bacterial cells inside Phaeocystis

In both 2019 and 2020, bacterial cells (fluorescent green) were

Table 2
P. globosa abundance, percentage of P. globosa cells in the <70 µm size fraction, and percentage of P. globosa cells <70 µm containing bacteria during the 2019 and 2020 spring bloom. P. globosa was absent in samples taken after the 8th of June 2020.

Date(y/m/d)	P. globosa abundance (10^3 cells mL^{-1})	P. globosa in <70 µm size fraction (%)	P. globosa cells with confirmed intracellular bacteria (%)	P. globosa cells with likely intracellular bacteria (%)
2019:				
19/05/02	27.7	75.8	0.6 - 2.0	1.5 – 3.7
2020:				
20/03/24	–	–	–	–
20/04/01	–	–	–	–
20/04/07	6.5	4.6	–	–
20/04/28	42.4	14.4	0.7	1.7
20/05/07	12.1	12.4	1.0	3.0
20/05/11	19.4	31.0	0.7	1.6
20/05/25	0.2	100	0.0	1.4
20/06/08	0.05	100	–	–

observed inside some of the red-stained *Phaeocystis* cells sampled from the spring bloom (Fig. 2; Table 2). Due to the double CARD-FISH hybridizations, much of the chlorophyll *a* was degraded, but its remaining red autofluorescence (chloroplasts) was still visible on both sides of the much more brightly fluorescent cytoplasm. Optical sectioning of a *Phaeocystis* cell into individual slices with the confocal microscope, to investigate the location of the bacteria, allowed visualization of the different fluorescent signals in each focal plane (Fig. 2A). The bacterial prey (indicated by the white arrow in Fig. 2A) comes into focus in the middle focal plane before disappearing again in the lower focal planes. A few *P. globosa* cells even contained two bacteria (Fig. 2B,C). A more detailed view of the localization of the bacterial prey was obtained from 3D reconstructions of the cell (see Supplementary Videos S1 and S2), clearly showing the bacterial cell being located inside the *Phaeocystis* cell. Here, a food vacuole seemed to be present, seen as a black circle surrounding the bacterial prey item. Moreover, localization of bacteria cells seemed to be highly consistent, with bacterial cells almost always being located along the longitudinal axis on one end of the cell, between the chloroplast and cytoplasm. This localization has also been seen in other haptophytes, in which prey items caught with the haptonema were brought to the posterior side of the cell where ingestion and digestion took place (Jones et al., 1993; Kawachi et al., 1991). However, because flagella could not be preserved and visualized reliably, the anterior or posterior side of the cell could not be determined in our study.

3.4. Incubation experiment

On the day of the 2019 incubation experiment (2nd of May), the surface water contained a low DIP concentration (0.04 µmol L^{-1}) and a high molar DIN:DIP ratio of 172, which is indicative of phosphorus limitation. In all four treatments of the incubation experiment, bacterial cells were observed inside some *P. globosa* cells (Fig. 3) with highest occurrences of intracellular bacteria observed 6 h after the start of the incubation (T_6) in the control treatment ($2.0 \pm 1.1\%$ of *P. globosa* cells). Lower percentages were observed for the nutrient amended ($+N + P$), dark, and nutrient amended $+$ dark treatments ($0.7 \pm 0.3\%$, $0.7 \pm 0.5\%$, and $0.6 \pm 0.3\%$, respectively; Fig. 3). However, statistical analysis of these results by a two-way ANOVA did not reveal significant main effects of the nutrient amendment ($F_{1,8} = 3.74$, $p = 0.09$) or the dark treatment ($F_{1,8} = 2.97$, $p = 0.12$) on the percentage of *Phaeocystis* cells containing bacteria. When counts of likely intracellular bacteria were added to the counts of bacteria with confirmed intracellular location, total percentage of potentially feeding *P. globosa* cells was higher for all four treatments, but again yielded no significant main effect of nutrient amendment ($F_{1,8} = 3.01$, $p = 0.12$) or dark treatment ($F_{1,8} = 2.88$, $p = 0.13$). Comparison of the control filters taken at noon (T_6) with those taken at midnight (T_{18}, data not shown) resulted in a similar percentage of potentially feeding cells at both time points ($1.38 \pm 0.21\%$; Student's

t-test, $t_4 = 0.91$, $p = 0.41$), indicating that there was no distinct diurnal variation in bacterial ingestion. The percentages of *P. globosa* cells containing bacteria in the 2019 incubation experiment were in the same range as the percentages found in the field samples from the 2020 spring bloom (Table 2).
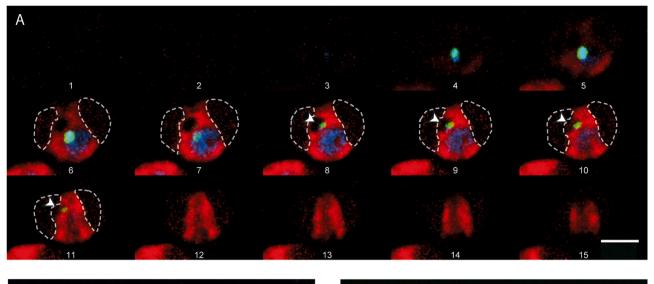
3.5. Mixotrophy predictions for Phaeocystis and other haptophyte lineages

The trophic strategies of 7 *Phaeocystis* and 24 other haptophyte strains were predicted using the gene-based model (Fig. 4). As expected, high photosynthesis prediction probabilities (generally > 0.8) were found in all strains assessed, while there was variability in the phagocytosis predictions. Two of the *Phaeocystis* strains, *P. cordata* RCC 1383 and *P. rex* CCMP2000, had a low phagocytosis prediction probability (0.02 and 0.12, respectively), which is indicative of a purely photoautotrophic lifestyle. In contrast, *P. globosa* CCMP1528 and the three *P. antarctica* strains (CCMP1374, Caron Lab Isolate, Rizkallah) all had high phagocytosis prediction probabilities, making the presence of a mixotrophic feeding strategy in these four strains highly likely. The last strain, *Phaeocystis* sp. CCMP2710, had intermediate prediction probabilities for both photosynthesis (0.63) and phagocytosis (0.46), perhaps due to a relatively low BUSCO completeness, suggesting that it might be a mixotroph as well.

Aside from the Phaeocystales, high prediction probabilities for both photosynthesis and phagocytosis, indicative of a mixotrophic feeding strategy, were obtained for the Isochrysidales (8 out of 9 species; phagocytosis probability ranging from 0.77 – 0.93), and the one Zygodiscales (0.96), three Coccolithales (0.79 – 0.94) and seven Prymnesiales (0.85 – 0.99) included in the analysis (Fig. 4). One exception was *E. huxleyi* CCMP374, for which a phagocytosis prediction probability of 0.02 was obtained, indicating that it is a purely photoautotrophic strain. For the Pavlovales, only *Pavlova* sp. CCMP459 was identified as a potential phago-mixotroph, with a phagocytosis prediction probability of 0.84. Several haptophytes (particularly Isochrysidales) could not be identified as phagotrophs by the full model, but were identified as such by the *R. allomycis* parasite model that used a lower number of conserved protein clusters predictive of phagocytosis (indicated by asterisks in Fig. 4; see Supplementary Figure S2).

4. Discussion

During the *Phaeocystis* spring blooms of two consecutive years we observed bacterial cells inside *P. globosa* cells. The intracellular bacteria appeared to be located in food vacuoles. Given the accompanying nutrient deplete conditions we suggest that these observations are an indication of phagotrophic feeding on bacteria, although more stable associations of *P. globosa* with bacteria (e.g. parasitism, symbiosis)
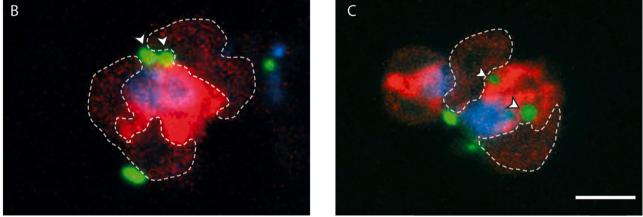
Fig. 2. Examples of *P. globosa* with bacterial cells inside. (A) Z-stack montage of a *P. globosa* cell containing a bacterium (fluorescent green). The photos show a complete stack of the same *P. globosa* cell, containing one intracellular bacterium, separated in individual slices. (B, C) Examples in which more than one bacterial cell was observed inside *P. globosa*. Cytoplasm is stained with Alexa Fluor™ 555 (red); nucleus is stained with DAPI (blue); chloroplasts are visible by the weak chlorophyll *a* autofluorescence (red) indicated by the dashed outline; bacteria are stained with Alexa Fluor™ 488 (green). Intracellular bacteria are highlighted by white arrows. Scale bar is 3 μm.

cannot be excluded. Further support for a phago-mixotrophic lifestyle in *P. globosa*, as well as other *Phaeocystis* species, was obtained from a gene-based predictive model. Earlier speculation about mixotrophy in *P. antarctica* was based on the transcriptional upregulation of genes involved in cytoskeleton structures and motility under micronutrient limitation (Rizkallah et al., 2020). This speculation was corroborated further by the recovery of *P. antarctica* sequence reads in the labeled DNA pool derived from feeding experiments using BrdU-labeled bacteria, although indirect routes of label incorporation could not be excluded (Gast et al., 2018). Our observations of bacteria-containing vacuoles in *P. globosa* and prediction of phagotrophic capability in several strains thus strongly support a potential for mixotrophy in *Phaeocystis* spp.

4.1. Potential grazing rates and impact on bacterial populations

The percentage of *P. globosa* cells containing bacteria was relatively low, in the range of 0.6 to 2%. Assuming these observations represent phagotrophic feeding by *Phaeocystis*, the impact on the bacterial community can be estimated. Using a conservative digestion time of ~1 h (Sherr et al., 1988; Thurman et al., 2010) and taking into account that the CARD-FISH probes covered only about 50% of the prokaryotic community, the average ingestion rate of *P. globosa* can be estimated at

0.012–0.040 bacteria cell^{-1} h^{-1}. If this is extended by adding the potential ingestion events in which the localization of bacterial cells inside *P. globosa* was less certain, a maximum rate of 0.08 bacteria cell^{-1} h^{-1} would be achieved. These estimated 'ingestion rates' are comparable to rates of 0.01–0.09 prey cell^{-1} h^{-1} achieved by several coccolithophores (Avrahami and Frada, 2020), but are much lower than reported for well-known mixotrophic haptophytes such as *Isochrysis galbana* (~1.0 bacteria cell^{-1} h^{-1}, Anderson et al., 2018), *Prymnesium patelliferum* (0 – 1.2 bacteria cell^{-1} h^{-1}, Legrand et al., 2001), *P. parvum* (3.4 – 5.8 bacteria cell^{-1} h^{-1}, Nygaard and Tobiesen, 1993) and *Chrysochromulina ericina* (8 - 18 bacteria cell^{-1} h^{-1}, Nygaard and Tobiesen, 1993).

Assuming the entire *P. globosa* population to be capable of mixotrophy, our estimates indicate that 24–96% of the population will have fed on at least one bacterial prey item over the course of a day. With abundances of 2×10^4 cells mL^{-1} for *P. globosa* and 2×10^6 cells mL^{-1} for the bacterial community, this would cause only a loss of 0.25–1.00% of the bacterial standing stock per day. While this loss is unlikely to have a significant impact on the bacterial community, these low ingestion rates could still play a role in *Phaeocystis'* bloom sustenance through acquisition of nutrients or growth factors from bacterial prey.
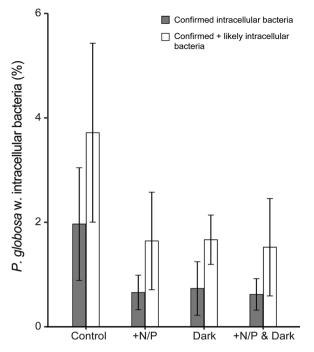
Fig. 3. Percentage of *P. globosa* cells with bacterial cells inside, for laboratory incubations under control conditions, nutrient amendment (+*N/P*), darkness, and the combination of darkness and nutrient amendment. Sampling time point is T_6 (noon). Bacteria were classified as "likely intracellular" if they appeared to be located inside *P. globosa* cells according to confocal microscopy, but alternative explanations (e.g., attachment to the cell surface) could not be excluded. Error bars represent ± 1 standard deviation (*n* = 3 replicates per treatment).

4.2. Nutrient limitation and its potential role in triggering bacterivory

Macronutrient limitation, especially by nitrogen and phosphorus, is often a trigger for feeding on bacterial prey by mixotrophs (Stoecker et al., 2017 and references therein). As bacteria are generally more competitive in the uptake of dissolved inorganic nutrients, these macronutrients become concentrated in the bacterial pool, thereby functioning as nutrient reservoir for nutrient-limited phagotrophic protists. Phosphorus appeared to be the limiting nutrient during both *Phaeocystis* blooms in this study, consistent with previous studies in the same area (Baudoux et al., 2006; Ly et al., 2014; Burson et al., 2016). Therefore, limitation by phosphorus was the most likely trigger for a potential feeding response. This is supported by a slightly decreased occurrence of bacterial cells inside *Phaeocystis* after nutrient amendment compared to the presumably P-limited control treatment, although this difference was not significant in our experiments (Fig. 3). Similarly, both dark treatments also showed a tendency to lower percentages of *P. globosa* cells with intracellular bacteria relative to the control. If this can be confirmed, it may further indicate that P-acquisition via phagocytosis supports nutrient requirements of a mainly photosynthetic lifestyle. Future experiments with axenic *P. globosa* cultures fed under different nutrient limiting conditions, as well as additional replication to enhance statistical power, could further aid in clarifying our observations and shed more light on the environmental triggers for feeding by *Phaeocystis*.

To estimate if feeding on bacteria could relieve phosphorus limitation of *Phaeocystis*, the P yield from ingesting one bacterial prey per day (0.04 bacteria cell^{-1} h^{-1}) was estimated. Using average biovolumes for bacteria in the North Sea ranging between 0.067 and 0.285 µm^3 (van Duyl et al., 1990; van Duyl and Kop, 1994) in combination with a carbon-to-volume equation (Menden-Deuer and Lessard, 2000) and published P:C ratios (Fagerbakke et al., 1996), it can be estimated that one bacterial prey would deliver 0.001 to 0.003 pg P cell^{-1}. With a subsistence quota (i.e. the minimum cellular P content below which no

cell division can take place) for *P. globosa* ranging between 0.005 - 0.01 pg P cell^{-1} (Jahnke, 1989), feeding on just one bacterial prey per day would allow cell division after 2–10 days. While not sufficient to sustain high growth rates, even low bacterial ingestion rates might thus intensify *Phaeocystis* blooms or help sustain them for longer periods of time. Together with its ability to hydrolyze organic phosphates (Admiraal and Veldhuis, 1987) acquisition of P via phagocytosis of bacterial prey might therefore contribute to the competitive strength of *P. globosa* during P-limitation at the end of the spring bloom.

In addition to P-limitation, vitamin availability may be a driving force for bacterial feeding by *Phaeocystis*. Similar to many other haptophytes, *Phaeocystis globosa* is a known thiamin (vitamin B$_1$) auxotroph which lacks the HMP-synthase needed for biosynthesis of the thiamin precursor HMP (Gutowska et al., 2017; Peperzak et al., 2000). Low ingestion rates of thiamin-producing bacteria might thus fulfill their vitamin requirements, as has been shown for the chlorophyte *Nephroselmis pyriformis* and the haptophyte *Isochrysis galbana* (Anderson et al., 2018).

Based on these considerations, both P and vitamins obtained from the ingested bacteria might help to sustain the growth of these HAB-forming haptophytes. As such, feeding on bacterial prey by *Phaeocystis* could explain its ability to bloom later in the season under nutrient deplete conditions (e.g. at the end of spring). Moreover, it also offers a possible explanation of why *P. globosa* blooms have persisted or even increased in the southern North Sea over the last decades (Philippart et al., 2020), despite reduced inputs of nitrogen and especially phosphorus into these coastal waters (Burson et al., 2016).

4.3. Prediction for phagotrophy in Phaeocystis and other haptophyte species

The potential for mixotrophy in *Phaeocystis* was not only derived from the observation of intracellular bacteria by confocal microscopy, but also supported by the *in silico* gene-based predictive model. This model bases its predictions on a significant enrichment of protein clusters shared with protists with known trophic strategy. Assigning core genes to the trophic strategy of phagocytosis is still difficult (Burns et al., 2018; Labarre et al., 2021) and interpretation of the data should be done carefully. Moreover, predicting phagotrophic potential of mixotrophic protists from transcriptome assemblies might not always be possible even if BUSCO scores are high, as many mixotrophs might express their phagocytotic machinery only under specific environmental conditions (e.g., nutrient limitation). Still, when combined with support from experimental evidence of ingested cells, as recently presented for several green algal species (Bock et al., 2021) and here for *P. globosa*, the model can be of substantial added value to identify potential mixotrophs.

Besides the Phaeocystales, the model predicted a phago-mixotrophic nutritional strategy for a variety of other species across the major lineages of haptophytes. In addition to the previously reported potential for mixotrophy in the coccolithophores *Calcidiscus leptoporus* and *Coccolithus pelagicus* ssp. *braarudi* (Houdan et al., 2006; Avrahami and Frada, 2020), the model resulted in three novel predictions for phago-mixotrophy in the coccolithophores *Gephyrocapsa oceanica*, *Scyphosphaera apsteinii* and *Pleurochrysis carterae*. Furthermore, strong phagotrophy predictions were obtained for several strains of *E. huxleyi* and *Isochrysis*, which is in accordance with earlier reports of phagotrophic feeding in these species (Rokitta et al., 2011; Anderson et al., 2018; Avrahami and Frada, 2020). An exception to this was *E. huxleyi* CCMP374, which does not seem to be capable of phagotrophy at all. Although flexibility in the mixotrophic potential has been demonstrated in other protists, such as *Ochromonas* spp. (Terrado et al., 2017; Wilken et al., 2020), intraspecific variation in the presence versus absence of a trophic strategy is noteworthy. However, it is in line with the large genome variability among *E. huxleyi* strains that can differ substantially in their metabolic repertoire (Read et al., 2013). Furthermore, phagocytosis in *E. huxleyi* and *Isochrysis* sp. was not predicted by the generalist
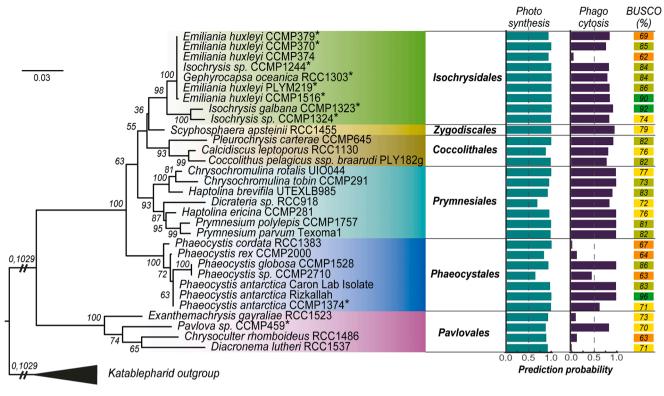
Fig. 4. Predicted potential for photosynthesis and phagocytosis among haptophytes. The data are presented as a maximum likelihood phylogenetic tree based on 18S rRNA sequences showing the major lineages of the haptophytes. The prediction probabilities for photosynthesis and phagocytosis of each strain are calculated from their sequenced genome or transcriptome by a gene-based predictive model (Burns et al., 2018). A probability greater than 0.5 is indicative of the presence of that trophic mode. Those strains for which phagotrophy was not predicted by the full model, but only by the reduced *R. allomycis* parasite model are indicated by an asterisk (see also Supplementary Figure S2). BUSCO% quantifies the completeness of the transcriptome assemblies and was subdivided in 10% categories as indicated by the different colours. Strains with a BUSCO coverage less than 60% were removed from the prediction model and phylogenetic tree.

model, but only by the model based on the intracellular parasite *R. allomycis*, which phagocytes host cytoplasm (Powell et al., 2017) and has a reduced number of genes involved in phagocytosis compared to generalist free-living phagocytotic protists. In particular, *R. allomycis* has lost genes related in actin filament organization, like WASH complexes or protein abpB (Burns et al., 2018). It remains an open question whether the generalist model fails to predict phagocytosis in phagotrophic Isochrysidales, due to (i) a distinct phagocytotic machinery not being captured by the generalist model, (ii) phagotrophy not being fully expressed at the time of transcriptome sampling, or (iii) due to a reduced core set of genes being retained in these mixotrophic species which, similar to *R. allomycis*, do not rely exclusively on phagocytosis for their nutrition. The latter might also lead to a loss of the capability for phagotrophy, as presumably is the case for *E. huxleyi* CCMP374. However, complete genome sequences will be needed to shed further light on the potential reduction or loss of phagocytotic machinery among members of the Isochrysidales.

The model further predicted the presence of a mixotrophic feeding strategy in seven species of the Prymnesiales as well as one species within the Pavlovales. For the majority of the investigated Prymnesiales and Pavlovales, the prediction by the gene-based model matches previous experimental observations (e.g. Jones et al., 1993; Havskum and Riemann, 1996; Hansen and Hjorth, 2002; Liu et al., 2015, 2016), with the exception of *Chrysochromulina rotalis* UIO044, and *Exanthemachrysis gayraliae* RCC1523. *C. tobin* CCMP291 had already been included as phago-mixotroph in the training set of the model (Burns et al., 2018), while *C. rotalis* was identified as phago-mixotroph by the model, in line with mixotrophy being common in this genus. Nevertheless, experimental evidence for phagotrophy is still lacking for these two species, although *C. tobin* had been claimed to be mixotrophic before (Hovde et al., 2015). In contrast, for *Exanthemachrysis* no support for

phagotrophy was obtained by the model. While this genus has been described as mixotrophic by Faure et al. (2019) and Schneider et al. (2020), supporting experimental evidence could not be traced from the literature cited in these two studies. *E. gayraliae* might therefore still be considered a pure photoautotroph until experimental evidence proves otherwise.

4.4. Ecological role of mixotrophy in haptophytes

While our model predictions suggest that mixotrophy is widespread across the haptophytes, their nutritional strategies likely differ substantially among taxa. Long recognized mixotrophs such as the HAB genera *Chrysochromulina* and *Prymnesium* show high ingestion rates of bacteria (8 - 18 and 3.4 - 5.8 bacteria cell^{-1} h^{-1}, respectively; Nygaard and Tobiesen, 1993) and can also feed on eukaryotic microalgae and even larger protists such as dinoflagellates and ciliates (Jones et al., 1993; Hansen and Hjorth, 2002; Tillmann 1998; 2003), thereby acquiring a substantial part of their carbon, nitrogen and phosphorus budgets via phagotrophy, even if these nutrients are sufficiently available in dissolved inorganic form (Carvalho and Granéli, 2010). This suggests that phagotrophy plays a vital role in the bloom development of *Chrysochromulina* and *Prymnesium*, and they employ a more heterotrophic lifestyle compared to species showing much lower ingestion rates, such as estimated here for *P. globosa* as well as reported for several coccolithophores (Avrahami and Frada, 2020). In the latter taxa, phagotrophy cannot provide sufficient macronutrients to support maximum growth rates, but consistent feeding on bacterial prey could still provide just enough nutrients to complement a phototrophic lifestyle and support low growth rates sufficient for bloom sustenance. Such a strategy would thus primarily rely on photoautotrophic growth and might limit the selective advantage for a phagotrophic potential to a

confined time period of inorganic nutrient deficiency. This could explain why phagotrophy is not universally present in bloom forming *Emiliania* and *Phaeocystis* species, making these lineages potentially interesting models for the evolutionary loss of phagotrophy in photosynthetic eukaryotes.

4.5. Concluding remarks

The results presented in this study strongly suggest the presence of a phago-mixotrophic feeding strategy in several *Phaeocystis* species including *P. globosa*. In addition, the gene-based predictive model also identified several other haptophytes as phago-mixotrophs that were previously presumed to be purely photoautotrophic. Although these model predictions should still be experimentally validated for several taxa, it demonstrates the spread of the phago-mixotrophic strategy along the major lineages of haptophytes including several HAB-forming species. Considering the scale at which these blooms impact local and global biogeochemical cycles as well as their potential economic and ecological impacts, these findings stress the importance of studying the potential for mixotrophy to sustain harmful algal blooms.

Author contributions

SK, SW, CB and JH conceptualized the research. CP maintained the long-term monitoring station at the NIOZ jetty and provided the time-series data. SK and SW designed the incubation experiment, and performed the 2019 fieldwork. CB was responsible for the 2020 sampling. SK performed CARD-FISH and confocal microscopy, and analyzed the data. DL and RM performed the model analysis. SK and SW wrote the manuscript and all authors provided comments and approved of the final version of the article.

Declaration of Competing Interest

The authors declare that they have no known competing financial interests or personal relationships that could have appeared to influence the work reported in this paper.

Data availability

Data will be made available on request.

Supplementary materials

Supplementary material associated with this article can be found, in the online version, at doi:10.1016/j.hal.2022.102292.

References

Admiraal, W., Veldhuis, M., 1987. Determination of nucleosides and nucleotides in seawater by HPLC; application to phosphatase activity in cultures of the alga *Phaeocystis pouchetii*. Mar. Ecol. Prog. Ser. 36, 277–285. https://doi.org/10.3354/meps036277.

Altschul, S.F., Gish, W., Miller, W., Myers, E.W., Lipman, D.J., 1990. Basic local alignment search tool. J. Mol. Biol. 215 (3), 403–410. https://doi.org/10.1016/S0022-2836(05)80360-2.

Anderson, R., Charvet, S., Hansen, P.J., 2018. Mixotrophy in chlorophytes and haptophytes: effect of irradiance, macronutrient, micronutrient and vitamin limitation. Front. Microbiol. 9, 1–13. https://doi.org/10.3389/fmicb.2018.01704.

Avrahami, Y., Frada, M.J., 2020. Detection of phagotrophy in the marine phytoplankton group of the coccolithophores (Calcihaptophycidae, Haptophyta) during nutrient-replete and phosphate-limited growth. J. Phycol. 56 (4), 1103–1108. https://doi.org/10.1111/jpy.12997.

Baudoux, A.-.C., Noordeloos, A.M., Veldhuis, M.J.W., Brussaard, C.P.D., 2006. Virally induced mortality of *Phaeocystis globosa* during two spring blooms in temperate coastal waters. Aquat. Microb. Ecol. 44 (3), 207–217. https://doi.org/10.3354/ame044207.

Bird, D.F., Kalff, J., 1986. Bacterial grazing by planktonic lake algae. Science 231, 493–495. https://doi.org/10.1126/science.231.4737.493.

Blauw, A.N., Los, F.J., Huisman, J., Peperzak, L., 2010. Nuisance foam events and *Phaeocystis globosa* blooms in Dutch coastal waters analyzed with fuzzy logic. J. Mar. Syst. 83 (3–4), 115–126. https://doi.org/10.1016/j.jmarsys.2010.05.003.

Bobrow, M.N., Adler, K.E., Roth, A., 2002. Enhanced Catalyzed Reporter Deposition, 372. US Pat. - US 6, p. 937 B1.

Bock, N.A., Charvet, S., Burns, J., Gyaltshen, Y., Rozenberg, A., Duhamel, S., Kim, E., 2021. Experimental identification and in silico prediction of bacterivory in green algae. ISME J 15, 1987–2000. https://doi.org/10.1038/s41396-021-00899-w.

Brisbin, M.M., Mitarai, S., 2019. Differential gene expression supports a resource-intensive, defensive role for colony production in the bloom-forming haptophyte, *Phaeocystis globosa*. J. Eukaryot. Microbiol. 66 (5), 788–801. https://doi.org/10.1111/jeu.12727.

Brosius, J., Dull, T.J., Sleeter, D.D., Noller, H.F., 1981. Gene organization and primary structure of a ribosomal RNA operon from *Escherichia coli*. J. Mol. Biol. 148 (2), 107–127. https://doi.org/10.1016/0022-2836(81)90508-8.

Brussaard, C.P.D., Kuipers, B., Veldhuis, M.J.W., 2005a. A mesocosm study of *Phaeocystis globosa* population dynamics: I. Regulatory role of viruses in bloom control. Harmful Algae 4 (5), 859–874. https://doi.org/10.1016/j.hal.2004.12.015.

Brussaard, C.P.D., Mari, X., Bleijswijk, J.D.L.Van, Veldhuis, M.J.W., 2005b. A mesocosm study of *Phaeocystis globosa* (Prymnesiophyceae) population dynamics: II. Significance for the microbial community. Harmful Algae 4 (5), 875–893. https://doi.org/10.1016/j.hal.2004.12.012.

Burkholder, J.A.M., Glibert, P.M., Skelton, H.M., 2008. Mixotrophy, a major mode of nutrition for harmful algal species in eutrophic waters. Harmful Algae 8 (1), 77–93. https://doi.org/10.1016/j.hal.2008.08.010.

Burns, J.A., Pittis, A.A., Kim, E., 2018. Gene-based predictive models of trophic modes suggest Asgard archaea are not phagocytotic. Nat. Ecol. Evol. 2, 697–704. https://doi.org/10.1038/s41559-018-0477-7.

Burson, A., Stomp, M., Akil, L., Brussaard, C.P.D., Huisman, J., 2016. Unbalanced reduction of nutrient loads has created an offshore gradient from phosphorus to nitrogen limitation in the North Sea. Limnol. Oceanogr. 61 (3), 869–888. https://doi.org/10.1002/lno.10257.

Cadée, G.C., Hegeman, J., 2002. Phytoplankton in the Marsdiep at the end of the 20th century; 30 years monitoring biomass, primary production, and *Phaeocystis* blooms. J. Sea Res. 48 (2), 97–110. https://doi.org/10.1016/S1385-1101(02)00161-2.

Carvalho, W.F., Granéli, E., 2010. Contribution of phagotrophy versus autotrophy to *Prymnesium parvum* growth under nitrogen and phosphorus sufficiency and deficiency. Harmful Algae 9 (1), 105–115. https://doi.org/10.1016/j.hal.2009.08.007.

Decelle, J., Romac, S., Stern, R.F., Bendif, E.M., Zingone, A., Audic, S., Guiry, M.D., Guillou, L., Tessier, D., Le Gall, F., Gourvil, P., Dos Santos, A.L., Probert, I., Vaulot, D., de Vargas, C., Christen, R., 2015. PhytoREF: a reference database of the plastidial 16S rRNA gene of photosynthetic eukaryotes with curated taxonomy. Mol. Ecol. Resour. 15 (6), 1435–1445. https://doi.org/10.1111/1755-0998.12401.

Fagerbakke, K.M., Heldal, M., Norland, S., 1996. Content of carbon, nitrogen, oxygen, sulfur and phosphorus in native aquatic and cultured bacteria. Aquat. Microb. Ecol. 10 (1), 15–27. https://doi.org/10.3354/ame010015.

Faure, E., Not, F., Benoiston, A.S., Labadie, K., Ayata, S.-.D., 2019. Mixotrophic protists display contrasting biogeographies in the global ocean. ISME J. 13 (4), 1072–1083. https://doi.org/10.1038/s41396-018-0340-5.

Field, C.B., Behrenfeld, M.J., Randerson, J.T., Falkowski, P., 1998. Primary production of the biosphere: integrating terrestrial and oceanic components. Science 281 (5374), 237–240. https://doi.org/10.1126/science.281.5374.237.

Flynn, K.J., Mitra, A., Anestis, K., Anschütz, A.A., Calbet, A., Ferreira, G.D., Gypens, N., Hansen, P.J., John, U., Martin, J.L., Mansour, J.S., Maselli, M., Medić, N., Norlin, A., Not, F., Pitta, P., Romano, F., Saiz, E., Schneider, L.K., Stolte, W., Traboni, C., 2019. Mixotrophic protists and a new paradigm for marine ecology: where does plankton research go now? J. Plankton Res. 41 (4), 375–391. https://doi.org/10.1093/plankt/fbz026.

Flynn, K.J., Mitra, A., Glibert, P.M., Burkholder, J.M., 2018. Mixotrophy in harmful algal blooms: by whom, on whom, when, why, and what next. In: Glibert, P.M. (Ed.), Global Ecology and Oceanography of Harmful Algal Blooms. Springer International Publishing AG, part of Springer Nature, pp. 113–132. https://doi.org/10.1007/978-3-319-70069-4_7.

Flynn, K.J., Stoecker, D.K., Mitra, A., Raven, J.A., Glibert, P.M., Hansen, P.J., Burkholder, J.M., 2013. Misuse of the phytoplankton-zooplankton dichotomy: the need to assign organisms as mixotrophs within plankton functional types. J. Plankton Res. 35 (1), 3–11. https://doi.org/10.1093/plankt/fbs062.

Gast, R.J., Fay, S.A., Sanders, R.W., 2018. Mixotrophic activity and diversity of Antarctic marine protists in austral summer. Front. Mar. Sci. 5, 1–12. https://doi.org/10.3389/fmars.2018.00013.

Gerea, M., Queimaliños, C., Schiaffino, M.R., Izaguirre, I., Forn, I., Massana, R., Unrein, F., 2013. *In situ* prey selection of mixotrophic and heterotrophic flagellates in Antarctic oligotrophic lakes: an analysis of the digestive vacuole content. J. Plankton Res. 35 (1), 201–212. https://doi.org/10.1093/plankt/fbs085.

Grasshoff, K., 1983. Determination of nitrite. In: Grasshoff, K., Ehrhardt, M., Kremling, K. (Eds.), Methods in Seawater Analysis. Wiley-VCH, Weinheim.

Guillard, R.R.L., Hargraves, P.E., 1993. *Stichochrysis immobilis* is a diatom, not a chrysophyte. Phycologia 32 (3), 234–236. https://doi.org/10.2216/i0031-8884-32-3-234.1.

Guillou, L., Bachar, D., Audic, S., Bass, D., Berney, C., Bittner, L., Boutte, C., Burgaud, G., De Vargas, C., Decelle, J., Del Campo, J., Dolan, J.R., Dunthorn, M., Edvardsen, B., Holzmann, M., Kooistra, W.H.C.F., Lara, E., Le Bescot, N., Logares, R., Mahé, F., Massana, R., Montresor, M., Morard, R., Not, F., Pawlowski, J., Probert, I., Sauvadet, A.L., Siano, R., Stoeck, T., Vaulot, D., Zimmermann, P., Christen, R., 2013. The protist ribosomal reference database (PR2): a catalog of unicellular eukaryote Small Sub-Unit rRNA sequences with curated taxonomy. Nucleic Acids Res. 41 (D1), 597–604. https://doi.org/10.1093/nar/gks1160.

Gutowska, M.A., Shome, B., Sudek, S., McRose, D.L., Hamilton, M., Giovannoni, S.J., Begley, T.P., Worden, A.Z., 2017. Globally important haptophyte algae use exogenous pyrimidine compounds more efficiently than thiamin. MBio 8 (5), 1–12. https://doi.org/10.1128/mBio.01459-17.

Hansen, P.J., Hjorth, M., 2002. Growth and grazing responses of *Chrysochromulina ericina* (Prymnesiophyceae): the role of irradiance, prey concentration and pH. Mar. Biol. 141 (5), 975–983. https://doi.org/10.1007/s00227-002-0879-5.

Havskum, H., Riemann, B., 1996. Ecological importance of bacterivorous, pigmented flagellates (mixotrophs) in the Bay of Aarhus, Denmark. Mar. Ecol. Prog. Ser. 137 (1–3), 251–263. https://doi.org/10.3354/meps137251.

Helder, W., de Vries, R.T.P., 1979. An automatic phenol-hypochlorite method for the determination of ammonia in sea- and brackish waters. Neth. J. Sea Res. 13 (1), 154–160. https://doi.org/10.1016/0077-7579(79)90038-3.

Hofeneder, H., 1930. Über die animalische Ernährung von *Ceratium hirundinella* O.F. Muller und über die Rolle des Kernes bei dieser Zellfunktion. Arch. Protistenk. 71, 1–32.

Houdan, A., Probert, I., Zatylny, C., Véron, B., Billard, C., 2006. Ecology of oceanic coccolithophores. I. Nutritional preferences of the two stages in the life cycle of *Coccolithus braarudii* and *Calcidiscus leptoporus*. Aquat. Microb. Ecol. 44 (3), 291–301. https://doi.org/10.3354/ame044291.

Hovde, B.T., Deodato, C.R., Hunsperger, H.M., Ryken, S.A., Yost, W., Jha, R.K., Patterson, J., Monnat, R.J., Barlow, S.B., Starkenburg, S.R., Cattolico, R.A., 2015. Genome sequence and transcriptome analyses of *Chrysochromulina tobin*: metabolic tools for enhanced algal fitness in the prominent order Prymnesiales (Haptophyceae). PLoS Genet 11 (9), 1–31. https://doi.org/10.1371/journal.pgen.1005469.

Huang, C.J., Dong, Q.X., Zheng, L., 1999. Taxonomic and ecological studies on a large scale *Phaeocystis pouchetii* bloom in the southeast coast of China during late 1997. Oceanol. Limnol. Sin. 30, 581–592.

Jacobs, P., Kromkamp, J.C., van Leeuwen, S.M., Philippart, C.J.M., 2020. Planktonic primary production in the western Dutch Wadden sea. Mar. Ecol. Prog. Ser. 639, 53–71. https://doi.org/10.3354/meps13267.

Jahnke, J., 1989. The light and temperature dependence of growth rate and elemental composition of *Phaeocystis globosa* scherffel and *P. pouchetii* (HAR.) Lagerh. in batch cultures. Neth. J. Sea Res. 23 (1), 15–21. https://doi.org/10.1016/0077-7579(89)90038-0.

Jones, H.L.J., Leadbeater, B.S.C., Green, J.C., 1993. Mixotrophy in marine species of *Chrysochromulina* (Prymnesiophyceae): ingestion and digestion of a small green flagellate. J. Mar. Biol. Assoc. 73 (2), 283–296. https://doi.org/10.1017/S0025315400032859. United Kingdom.

Jones, R.I., 2000. Mixotrophy in planktonic protists: an overview. Freshw. Biol. 45 (2), 219–226. https://doi.org/10.1046/j.1365-2427.2000.00672.x.

Kawachi, M., Inouye, I., Maeda, O., Chihara, M., 1991. The haptonema as a food-capturing device: observations on *Chrysochromulina hirta* (Prymnesiophyceae). Phycologia 30 (6), 563–573. https://doi.org/10.2216/i0031-8884-30-6-563.1.

Keeling, P.J., Burki, F., Wilcox, H.M., Allam, B., Allen, E.E., Amaral-Zettler, L.A., Armbrust, E.V., Archibald, J.M., Bharti, A.K., Bell, C.J., Beszteri, B., Bidle, K.D., Cameron, C.T., Campbell, L., Caron, D.A., Cattolico, R.A., Collier, J.L., Coyne, K., Davy, S.K., Deschamps, P., Dyhrman, S.T., Edvardsen, B., Gates, R.D., Gobler, C.J., Greenwood, S.J., Guida, S.M., Jacobi, J.L., Jakobsen, K.S., James, E.R., Jenkins, B., John, U., Johnson, M.D., Juhl, A.R., Kamp, A., Katz, L.A., Kiene, R., Kudryavtsev, A., Leander, B.S., Lin, S., Lovejoy, C., Lynn, D., Marchetti, A., McManus, G., Nedelcu, A. M., Menden-Deuer, S., Miceli, C., Mock, T., Montresor, M., Moran, M.A., Murray, S., Nadathur, G., Nagai, S., Ngam, P.B., Palenik, B., Pawlowski, J., Petroni, G., Piganeau, G., Posewitz, M.C., Rengefors, K., Romano, G., Rumpho, M.E., Rynearson, T., Schilling, K.B., Schroeder, D.C., Simpson, A.G.B., Slamovits, C.H., Smith, D.R., Smith, G.J., Smith, S.R., Sosik, H.M., Stief, P., Theriot, E., Twary, S.N., Umale, P.E., Vaulot, D., Wawrik, B., Wheeler, G.L., Wilson, W.H., Xu, Y., Zingone, A., Worden, A.Z., 2014. The marine microbial eukaryote transcriptome sequencing project (MMETSP): illuminating the functional diversity of eukaryotic life in the oceans through transcriptome sequencing. PLoS Biol. 12 (6), 1–6. https://doi.org/10.1371/journal.pbio.1001889.

Kumar, S., Stecher, G., Li, M., Knyaz, C., Tamura, K., 2018. MEGA X: molecular evolutionary genetics analysis across computing platforms. Mol. Biol. Evol. 35 (6), 1547–1549. https://doi.org/10.1093/molbev/msy096.

Labarre, A., López-Escardó, D., Latorre, F., Leonard, G., Bucchini, F., Obiol, A., Cruaud, C., Sieracki, M.E., Jaillon, O., Wincker, P., Vandepoele, K., Logares, R., Massana, R., 2021. Comparative genomics reveals new functional insights in uncultured MAST species. ISME J. 15 (6), 1767–1781. https://doi.org/10.1038/s41396-020-00885-8.

Lancelot, C., 1995. The mucilage phenomenon in the continental coastal waters of the North Sea. Sci. Total Environ. 165 (1–3), 83–102. https://doi.org/10.1016/0048-9697(95)04545-C.

Lange, M., Guillou, L., Vaulot, D., Simon, N., Amann, R.I., Ludwig, W., Medlin, L.K., 1996. Identification of the class Prymnesiophyceae and the genus *Phaeocystis* with ribosomal RNA-targeted nucleic acid probes detected by flow cytometry. J. Phycol. 32 (5), 858–868. https://doi.org/10.1111/j.0022-3646.1996.00858.x.

Legrand, C., Johansson, N., Johnsen, G., Borsheim, K.Y., Granéli, E., 2001. Phagotrophy and toxicity variation in the mixotrophic *Prymnesium patelliferum* (Haptophyceae). Limnol.Oceanogr 46 (5), 1208–1214. https://doi.org/10.4319/lo.2001.46.5.1208.

Liu, Z., Koid, A.E., Terrado, R., Campbell, V., Caron, D.A., Heidelberg, K.B., 2015. Changes in gene expression of *Prymnesium parvum* induced by nitrogen and phosphorus limitation. Front. Microbiol. 6, 1–13. https://doi.org/10.3389/fmicb.2015.00631.

Liu, Z., Campbell, V., Heidelberg, K.B., Caron, D.A., 2016. Gene expression characterizes different nutritional strategies among three mixotrophic protists. FEMS Microbiol. Ecol. 92 (7), 1–11. https://doi.org/10.1093/femsec/fiw106.

Ly, J., Philippart, C.J.M., Kromkamp, J.C., 2014. Phosphorus limitation during a phytoplankton spring bloom in the western Dutch Wadden Sea. J. Sea Res. 88, 109–120. https://doi.org/10.1016/j.seares.2013.12.010.

Manz, W., Amann, R., Ludwig, W., Wagner, M., Schleifer, K.H., 1992. Phylogenetic oligodeoxynucleotide probes for the major subclasses of Proteobacteria: problems and solutions. Syst. Appl. Microbiol. 15 (4), 593–600. https://doi.org/10.1016/S0723-2020(11)80121-9.

Manz, W., Amann, R., Ludwig, W., Vancanneyt, M., Schleifer, K.H., 1996. Application of a suite of 16S rRNA-specific oligonucleotide probes designed to investigate bacteria of the phylum cytophaga-flavobacter-bacteroides in the natural environment. Microbiology 142 (5), 1097–1106. https://doi.org/10.1099/13500872-142-5-1097.

Menden-Deuer, S., Lessard, E.J., 2000. Carbon to volume relationships for dinoflagellates, diatoms, and other protist plankton. Limnol. Oceanogr. 45 (3), 569–579. https://doi.org/10.4319/lo.2000.45.3.0569.

Mitra, A., Flynn, K.J., Burkholder, J.M., Berge, T., Calbet, A., Raven, J.A., Granéli, E., Glibert, P.M., Hansen, P.J., Stoecker, D.K., Thingstad, F., Tillmann, U., Väge, S., Wilken, S., Zubkov, M.V., 2014. The role of mixotrophic protists in the biological carbon pump. Biogeosciences 11 (4), 995–1005. https://doi.org/10.5194/bg-11-995-2014.

Murphy, J., Riley, J.P., 1962. A modified single solution method for the determination of phosphate in natural waters. Anal. Chim. Acta 27, 31–36. https://doi.org/10.1057/9781137461131.

Nygaard, K., Tobiesen, A., 1993. Bacterivory in algae: a survival strategy during nutrient limitation. Limnol. Oceanogr. 38 (2), 273–279. https://doi.org/10.4319/lo.1993.38.2.0273.

Pascher, A., 1917. Flagellaten und Rhizopoden in ihren gegenseitigen Beziehungen. Arch. Protistenk. 38, 1–87.

Peperzak, L., Gieskes, W.W.C., Colijn, F., 2000. The vitamin B requirement of *Phaeocystis globosa* (Prymnesiophyceae). J. Plankton Res. 22 (8), 1529–1537. https://doi.org/10.1093/plankt/22.8.1529.

Pernthaler, A., Amann, R., 2004. Simultaneous fluorescence in situ hybridization of mRNA and rRNA in environmental bacteria. Appl. Environ. Microbiol. 70 (9), 5426–5433. https://doi.org/10.1128/AEM.70.9.5426.

Philippart, C.J., Cadée, G.C., van Raaphorst, W., Riegman, R., 2000. Long-term phytoplankton-nutrient interactions in a shallow coastal sea: algal community structure, nutrient budgets, and denitrification potential. Limnol. Oceanogr. 45 (1), 131–144. https://doi.org/10.4319/lo.2000.45.1.0131.

Philippart, C.J., Blauw, A., Bolhuis, H., Brandenburg, K., Brussaard, C.P.D., Gerkema, T., Herman, P., Hommersom, A., Jacobs, P., Laanen, M., van Leeuwe, M.A., van den Oever, A., Peters, S., Philippart, M., Pitarch, J., Prins, T., Ruddick, K., Spaias, L., van de Waal, D., Van der Zande, D., Zuur, A., 2020. Quick Scan Zeeschuim. Technische Universiteit Delft (TUD), Universiteit van Amsterdam (UvA), Universiteit Utrecht (UU), Rijksuniversiteit Groningen (RUG) & Water Insight BV, Texel. Rapport van het Koninklijk Nederlands Instituut voor Onderzoek der Zee (NIOZ-NWO), Bureau Waardenburg BV, Deltares, Highland Statistics, Italian National Research Council (CNR), Koninklijk Belgisch Instituut voor Natuurwetenschappen (KBIN), Nederlands Instituut voor Ecologie (NIOO-KNAW), Rijkswaterstaat (RWS-WVL)mei 2020. https://www.deltares.nl/app/uploads/2020/06/Quick-Scan-ZEESCHUIM-DEF-2-juni-2020.pdf.

Piwosz, K., Mukherjee, I., Salcher, M.M., Grujčić, V., Šimek, K., 2021. CARD-FISH in the sequencing era: opening a new universe of protistan ecology. Front. Microbiol. 12, 1–24. https://doi.org/10.3389/fmicb.2021.640066.

Powell, M.J., Letcher, P.M., James, T.Y., 2017. Ultrastructural characterization of the host-parasite interface between *Allomyces anomalus* (Blastocladiomycota) and *Rozella allomycis* (Cryptomycota). Fungal Biol. 121, 561–572. https://doi.org/10.1016/j.funbio.2017.03.002.

Quast, C., Pruesse, E., Yilmaz, P., Gerken, J., Schweer, T., Yarza, P., Peplies, J., Glöckner, F.O., 2013. THE SILVA ribosomal RNA gene database project: improved data processing and web-based tools. Nucleic Acids Res. 41 (D1), 590–596. https://doi.org/10.1093/nar/gks1219.

Raven, J.A., 1997. Phagotrophy in phototrophs. Limnol. Oceanogr. 42 (1), 198–205. https://doi.org/10.4319/lo.1997.42.1.0198.

Read, B.A., Kegel, J., Klute, M.J., Kuo, A., Lefebvre, S.C., Maumus, F., Mayer, C., Miller, J., Monier, A., Salamov, A., Young, J., Aguilar, M., Claverie, J.M., Frickenhaus, S., Gonzalez, K., Herman, E.K., Lin, Y.C., Napier, J., Ogata, H., Sarno, A. F., Shmutz, J., Schroeder, D., De Vargas, C., Verret, F., Von Dassow, P., Valentin, K., Van De Peer, Y., Wheeler, G., Dacks, J.B., Delwiche, C.F., Dyhrman, S.T., Glöckner, G., John, U., Richards, T., Worden, A.Z., Zhang, X., Grigoriev, I.V., 2013. Pan genome of the phytoplankton *Emiliania* underpins its global distribution. Nature 499, 209–213. https://doi.org/10.1038/nature12221.

Rizkallah, M.R., Frickenhaus, S., Trimborn, S., Harms, L., Moustafa, A., Benes, V., Gäbler-Schwarz, S., Beszteri, S., 2020. Deciphering patterns of adaptation and acclimation in the transcriptome of *Phaeocystis antarctica* to changing iron conditions. J. Phycol. 56 (3), 747–760. https://doi.org/10.1111/jpy.12979.

Rokitta, S.D., de Nooijer, L.J., Trimborn, S., de Vargas, C., Rost, B., John, U., 2011. Transcriptome analyses reveal differential gene expression patterns between the life-cycle stages of *Emiliania huxleyi* (Haptophyta) and reflect specialization to different ecological niches. J. Phycol. 47 (4), 829–838. https://doi.org/10.1111/j.1529-8817.2011.01014.x.

Savage, R.E., 1930. The influence of *Phaeocystis* on the migration of the herring. Fishery Invest. II 12 (2), 5–13.

Schindelin, J., Arganda-Carreras, I., Frise, E., Kaynig, V., Longair, M., Pietzsch, T., Preibisch, S., Rueden, C., Saalfeld, S., Schmid, B., Tinevez, J.Y., White, D.J., Hartenstein, V., Eliceiri, K., Tomancak, P., Cardona, A., 2012. Fiji: an open-source platform for biological-image analysis. Nat. Methods 9 (7), 676–682. https://doi.org/10.1038/nmeth.2019.

Schneider, L.K., Anestis, K., Mansour, J., Anschütz, A.A., Gypens, N., Hansen, P.J., John, U., Klemm, K., Martin, J.L., Medic, N., Not, F., Stolte, W., 2020. A dataset on trophic modes of aquatic protists. Biodivers. Data J. 8, e56648. https://doi.org/10.3897/BDJ.8.e56648.

Schoemann, V., Becquevort, S., Stefels, J., Rousseau, V., Lancelot, C., 2005. *Phaeocystis* blooms in the global ocean and their controlling mechanisms: a review. J. Sea Res. 53 (1–2), 43–66. https://doi.org/10.1016/j.seares.2004.01.008.

Seong, K.A., Jeong, H.J., Kim, S., Kim, G.H., Kang, J.H., 2006. Bacterivory by co-occurring red-tide algae, heterotrophic nanoflagellates, and ciliates. Mar. Ecol. Prog. Ser. 322, 85–97. https://doi.org/10.3354/meps322085.

Sherr, B.F., Sherr, E.B., Rassoulzadegan, F., 1988. Rates of digestion of bacteria by marine phagotrophic protozoa: temperature dependence. Appl. Environ. Microbiol. 54 (5), 1091–1095. https://doi.org/10.1128/aem.54.5.1091-1095.1988.

Stoecker, D.K., 1999. Mixotrophy among dinoflagellates. J. Eukaryot. Microbiol. 46 (4), 397–401. https://doi.org/10.1111/j.1550-7408.1999.tb04619.x.

Stoecker, D.K., Hansen, P.J., Caron, D.A., Mitra, A., 2017. Mixotrophy in the marine plankton. Ann. Rev. Mar. Sci. 9, 311–335. https://doi.org/10.1146/annurev-marine-010816-060617.

Strickland, J.D.H., Parsons, T.R., 1968. Determination of reactive silicate. In: Stevenson, J.C., Watson, J., Reinhart, J.M., Cook, D.G. (Eds.), A Practical Handbook of Seawater Analysis. Fisheries Research Board of Canada, Bulletin 167 (2nd edition), p. 65.

Terrado, R., Pasulka, A.L., Lie, A.A.Y., Orphan, V.J., Heidelberg, K.B., Caron, D.A., 2017. Autotrophic and heterotrophic acquisition of carbon and nitrogen by a mixotrophic chrysophyte established through stable isotope analysis. ISME J. 11 (9), 2022–2034. https://doi.org/10.1038/ismej.2017.68.

Thurman, J., Drinkall, J., Parry, J.D., 2010. Digestion of bacteria by the freshwater ciliate *Tetrahymena pyriformis*. Aquat. Microb. Ecol. 60 (2), 163–174. https://doi.org/10.3354/ame01413.

Tillmann, U., 1998. Phagotrophy of a plastidic haptophyte, *Prymnesium patelliferum*. Aquat. Microb. Ecol. 14, 155–160. https://doi.org/10.3354/ame014155.

Tillmann, U., 2003. Kill and eat your predator: a winning strategy of the planktonic flagellate *Prymnesium parvum*. Aquat. Microb. Ecol. 32, 73–84. https://doi.org/10.3354/ame032073.

van Duyl, F.C., Bak, R.P.M., Kop, A.J., Nieuwland, G., 1990. Bacteria, auto- and heterotrophic nanoflagellates, and their relations in mixed, frontal and stratified waters of the North Sea. Netherlands J. Sea Res. 26 (9), 97–109. https://doi.org/10.1016/0077-7579(90)90060-T.

van Duyl, F.C., Kop, A.J., 1994. Bacterial production in North Sea sediments: clues to seasonal and spatial variations. Mar. Biol. 120 (2), 323–337. https://doi.org/10.1007/BF00349694.

Veldhuis, M.J.W., Wassmann, P., 2005. Bloom dynamics and biological control of a high biomass HAB species in European coastal waters: a *Phaeocystis* case study. Harmful Algae 4 (5), 805–809. https://doi.org/10.1016/j.hal.2004.12.004.

Waterhouse, R.M., Seppey, M., Simão, F.A., Manni, M., Ioannidis, P., Klioutchnikov, G., Kriventseva, E.V., Zdobnov, E.M., 2018. BUSCO applications from quality assessments to gene prediction and phylogenomics. Mol. Biol. Evol. 35 (3), 543–548. https://doi.org/10.1093/molbev/msx319.

Weisse, T., Tande, K., Verity, P., Hansen, F., Gieskes, W., 1994. The trophic significance of *Phaeocystis* blooms. J. Mar. Syst. 5 (1), 67–79. https://doi.org/10.1016/0924-7963(94)90017-5.

Wilken, S., Choi, C.J., Worden, A.Z., 2020. Contrasting mixotrophic lifestyles reveal different ecological niches in two closely related marine protists. J. Phycol. 56 (1), 52–67. https://doi.org/10.1111/jpy.12920.

Worden, A.Z., Follows, M.J., Giovannoni, S.J., Wilken, S., Zimmerman, A.E., Keeling, P. J., 2015. Rethinking the marine carbon cycle: factoring in the multifarious lifestyles of microbes. Science 347 (6223), 1257594. https://doi.org/10.1126/science.1257594.

Zdobnov, E.M., Tegenfeldt, F., Kuznetsov, D., Waterhouse, R.M., Simao, F.A., Ioannidis, P., Seppey, M., Loetscher, A., Kriventseva, E.V., 2017. OrthoDB v9.1: cataloging evolutionary and functional annotations for animal, fungal, plant, archaeal, bacterial and viral orthologs. Nucleic Acids Res. 45 (1), 744–749. https://doi.org/10.1093/nar/gkw1119.

Zingone, A., Chrétiennot-Dinet, M.J., Lange, M., Medlin, L., 1999. Morphological and genetic characterization of *Phaeocystis cordata* and *P. jahnii* (Prymnesiophyceae), two new species from the Mediterranean Sea. J. Phycol. 35 (6), 1322–1337. https://doi.org/10.1046/j.1529-8817.1999.3561322.x.

Zubkov, M.V., Tarran, G.A., 2008. High bacterivory by the smallest phytoplankton in the North Atlantic Ocean. Nature 455, 224–226. https://doi.org/10.1038/nature07236.